LA-UR -87-2538

CONF 870810--1

Los Alamos National Laboratory is operated by the University of California for the United States Department of Energy under contract W-7405-ENG-36

TITLE METHOD FOR SINGLE-SHOT MEASUREMENT OF PICOSECOND LASER PULSE-LENGTHS WITHOUT ELECTRONIC TIME DISPERSION

LA-UR--87-2538

DE87 013171

AUTHOR(S) George A. Kyrala, P-1

SUBMITTED TO SPIE's 31st Annual International Technical Symposium
Town and Country Hotel
San Diego, California

August 16-21, 1987

DISCLAIMER

MASTER

Los Alamos Los Alamos National Laboratory
Los Alamos, New Mexico 87545

FORM NO. 836 R4
ST. NO. 2629 5/81

DISTRIBUTION OF THIS DOCUMENT IS UNLIMITED

Method for single-shot measurement of picosecond laser pulse-lengths without electronic time dispersion

George A. Kyrala

Los Alamos National Laboratory, Physics Division
P.O. Box 1663, MS E526, Los Alamos, New Mexico 87545

ABSTRACT

A two-source shear pattern recording is proposed as a method for single-shot measurement of the pulse shape from nearly monochromatic sources whose pulse lengths are shorter than their coherence times. The basis of this method relies on the assertion that if two identical electromagnetic pulses are recombined with a time delay greater than the sum of their pulse widths, the recordable spatial pattern has no fringes in it. At an arbitrary delay, translated into an actual spatial recording position, the recorded modulated intensity will sample the corresponding laser intensity at that delay time, but with a modulation due to the coherence function of the electromagnetic pulse. Two arrangements are proposed for recording the pattern. The principles, the design parameters, and the methodologies of these arrangements will be presented. Resolutions of the configurations and their limitations will be given as well.

1. INTRODUCTION

Short pulses of electromagnetic radiation can be characterized by their pulse width and their coherence time. Alternative quantities in the complementary domain are spectral bandwidth and spectral structure. The concept of coherence for a short pulse is physically hard to define, since the pulse duration is not long enough to describe the temporal coherence property of the pulse.[1] For a broadband pulse, white pulse, of duration $\Delta t = 1$ ps, the spectral frequency bandwidth $\Delta\nu$ is typically 10^{14} Hz. The Sampling theorem[2] allows for N_t temporal samples in the pulse, $N_t = \Delta\nu\ \Delta t \sim 10^2$. Thus statistical techniques must be applied to average in time. This is a consequence of the non-coherence of the light, and of its non fourier-transform limited nature. For laser light on the otherhand, the spectral bandwidth is of the order $\Delta\nu = 10^{12}$ Hz for a $\Delta t = 1$ ps pulse. Thus the number of temporal samples $N_t = 1$. Therefore, we have temporal coherence, or in alternative language we have a nearly-transform-limited electromagnetic pulse. The measurement of the short pulse properties fall into two broadband categories. For broadband light, streak cameras and photodetectors have been

applied to measure the light duration to the order of a picosecond. For monochromatic radiation in the visible and the infrared, autocorrelation techniques utilizing mixing in non-linear crystals[3] and dyes,[4] interferometric techniques,[5] scattering from self-induced transient diffraction grating,[6] two photon fluorescence,[7] two-photon excitation of recording film,[8] and multiphoton ionization.[9] For short wavelengths (λ < 250 nm) few of these techniques work. Streak cameras and detectors are limited to a picosecond pulse length by the spread in energy of the photoelectrons due to the large photoabsorption depths in the photocathodes. Correlation techniques using non-linear conversion, though applied successfully in at least one case,[10] are generally limited since the energy from two photon absorption ionizes most non-linear materials. Only multiphoton-ionization is of general use, however the technique does not work for single shot measurement of the pulse shape, and its signals are very dependent (N!) on the number of modes N in and the irradiance of the laser beam. The number of modes and the intensity may vary from shot to shot.

In this report a new twist on the interference method is presented and discussed. The method can be applied to any coherent oscillatory disturbance from the infrared to the x-rays region of the spectrum. Provided enough energy exists in a pulse for recording, the method is capable of single shot pulse shape measurement.

2. PRINCIPLE

The basic principle used here is splitting the incident pulse into two beams that travel different, but very close, paths, then allowing those two beams to interfere. The electric field strength, E_i within each pulse i can be expressed:[11]

$$E_i = \frac{1}{2} V_i(t + T_i) e^{i(\vec{K}_i \cdot \vec{r})} + cc \qquad (1)$$

where $\vec{K}_i$ is the wave vector, $\vec{r}$ is the position vector, and T_i is a delay time. The time dependent amplitude $V_i(t)$ will be expressed as a modulated signal of carrier mean frequency ω_o:

$$V_i(t) = A_i(t)\ e^{i[\phi_i(t) - \omega_o t]} \qquad (2)$$

where $A_i(t)$ and $\phi_i(t)$ vary slowly in comparison with ωt. When these pulses interfere, the recorded irradiance will be:

$$I = \int_{-\infty}^{\infty} |E_1 + E_2|^2 \, dt \tag{3}$$

$$= \frac{1}{2}\int |V_1(t)|^2 dt d\omega + \frac{1}{2}\int |V_2(t+T)|^2 dt$$

$$+ \int \left\{ V_1(t) V_2(t+T)^* e^{i(\vec{k}_1 - \vec{k}_2)\cdot\vec{x}} + cc \right\} dt \tag{4}$$

which for a monochromatic beam reduces to:

$$I = \frac{1}{2}\left[\Gamma_{11}(0) + \Gamma_{22}(0)\right] + \left\{ \Gamma_{12}(T)\ e^{i(\vec{k}_1 - \vec{k}_2)\cdot\vec{x}} + cc \right\} \tag{5}$$

where the temporal coherence function Γ is defined as:[11]

$$\Gamma_{12}(T) = \int_{-\infty}^{\infty} V_1(t+T) V_2(t)^* dt \tag{6}$$

One thus sees a modulated signal at a carrier frequency $(\vec{k}_1 - \vec{k}_2)\cdot\vec{x}$ with a much slower variation due to the coherence function Γ_{12}.

Two models for the coherence function can be advanced. The first gives a linear chirp in the phase of the disturbance, i.e., an exponential pulse:

$$V_\alpha(t) = \begin{cases} \exp(i\omega_0 t - \alpha t) & t \geq 0 \\ 0 & t < 0 \end{cases} \tag{7a}$$

The second gives a frequency chirped gaussian pulse:

$$V_\beta(t) = \exp\left(-\alpha t^2 + i(\omega_0 t - \beta t^2)\right) \tag{7b}$$

These two models lead to two physical spectral distributions Lorentzian and Gaussian respectively:

$$\frac{2}{T}\ \frac{1}{(\omega-\omega_o)^2+\left(\frac{1}{T}\right)^2} \tag{8a}$$

$G(w)$ =

$$T\sqrt{\pi}\ \exp\left[-(\omega-\omega_o)^2\ \frac{T^2}{4}\right] \tag{8b}$$

with spectral widths $\Delta\omega$ - $2/T.4\sqrt{\ln 2}/T$ research.

Since $G(\omega) = \int \left|\frac{\Gamma(T)}{\Gamma(0)}\right| e^{i\omega_o T - i\omega T} dT$ (9)

the models relate to the coherence functions:

$$e^{-T_1/T} = e^{-2\ln 2/t_c} \tag{10a}$$

$\Gamma(T)/\Gamma(0)$ =

$$e^{-T^2/T^2} = e^{-4\ln 2T^2/t_c^2} \tag{10b}$$

where the coherence time t_c is related to T as

$$2\ln 2 \quad T \tag{11a}$$

t_c =

$$2\sqrt{\ln 2} \quad T \tag{11b}$$

For these two models, rigorous relationships can be found between the coherence time t_c, and the pulse FWHM width t_p.[6]

$$\frac{\ln 2}{2a} = \frac{t_c}{4} \tag{12a}$$

t_p =

$$\sqrt{\frac{2\ln 2}{a}} = \frac{t_c}{2}\sqrt{1+\left(\frac{\beta}{a}\right)^2} \tag{12b}$$

It is important to note that in the exponential case (Case A) the coherence time of the pulse is longer than the pulse time. Equally important for the Gaussian pulse, the coherence time is larger than the pulse time, provided the frequency chirp is small. For a transform-limited Gaussian pulse, $\beta = 0$. Thus the present method for measuring pulse length rather than coherence length is justified.

3. TWO SLIT DESIGN

The two slit design is shown schematically in Figure 1. Essentially one is using the two slits to sample the incident pulse. In its simplest form, two spatially different parts of the pulse are sampled, in which case one is also sensitive to spatial coherence. By using diffraction from one slit to illuminate both slits, one samples the same region of the pulse area, limited to the signal to noise and the single slit area.[12] Using the standard formulation for diffraction from one slit, the electric field at the screen, due to a small width dy within the slit, will be:

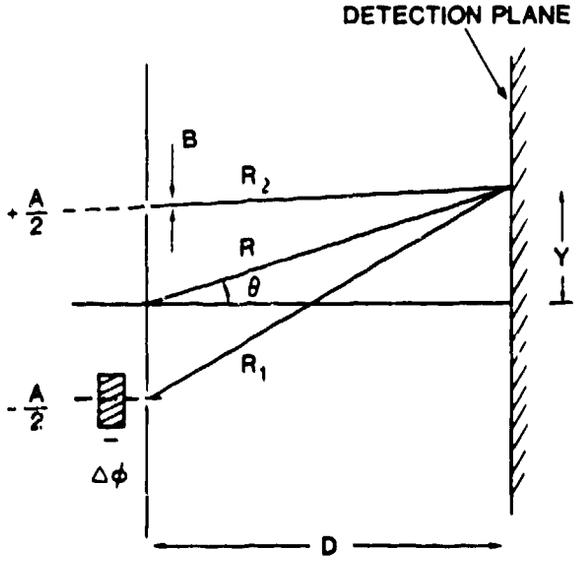

Figure 1. Geometry used for two slit interferometer.

$$dE(R,t) = \epsilon_1[\omega t - kR + \phi_1]\cos(\omega t - kR + \phi_1)\frac{dy}{R} \qquad (13)$$

Where ϕ is an arbitrary phase due to misalignment, etc., and $\omega t - kR$ is the optical path difference. Integrating over the slit width B,

$$E(R,t) = B \frac{\epsilon_1}{R} \frac{\sin\beta}{\beta} \cos(\omega t - kR + \phi_1) \tag{14}$$

where $\beta = \frac{kB \sin \phi}{2}$ (15)

Thus the recorded exposure is

$$I = \langle |E(R,t)|^2 \rangle_t = \frac{1}{2}\left[\frac{B}{R} \frac{\sin\beta}{\beta}\right]^2 \int_{-\infty}^{\infty} \epsilon_1^2(t)dt \tag{16}$$

For a normalized gaussian pulse shape in intensity with full width at half maximum FWHM = 1.66 σ_I, we write:

$$I(t) = \frac{1}{\sigma_I\sqrt{\pi}} \exp -\left(\frac{t}{\sigma_I}\right)^2 \tag{17}$$

a normalized function:

$$\int \epsilon_1^2(t)dt = \int I(t)dt = 1 \tag{18}$$

The corresponding electric field pulse shape is wider:

$$\epsilon_1(t) = \frac{1}{\sqrt{\sqrt{\pi}\sigma_I}} \exp\left(-\frac{t^2}{2\sigma_I^2}\right) \tag{19}$$

For two slits of width B separated by gap A, the electric field is the sum of the electric field from the two slits. Thus the irradiance is given by:

$$I = \langle |E|^2 \rangle = \langle |E_1|^2 \rangle + \langle |E_2|^2 \rangle + 2\langle E_1 E_2^* \rangle = I_1 + I_2 + I_c \tag{20}$$

where the first two terms are the regular irradiances due to diffraction from each slit while the last cross term can be treated simply:

$$I_c = 2\sqrt{I_1 I_2}\int_{-\infty}^{\infty} \epsilon_L\left[t-\frac{R_1}{c}+\phi_1\right]\epsilon_L^*\left(t-\frac{R_2}{c}+\phi_2\right)\cos(\omega t-kR_1+\phi_1)\cos(\omega t-kR_2+\phi_2)dt$$

$$= 2\sqrt{I_1 I_2}\cos(k(R_1-R_2)+(\phi_1-\phi_2))\int_{-\infty}^{\infty}\epsilon_{L1}\epsilon_{L2}\,dt \qquad (21)$$

$$= 2\sqrt{I_1 I_2}\cos(k\Delta R+\Delta\phi)\exp-\left(\frac{\Delta R}{2c\sigma_l}\right)^2$$

The total irradiance will be cast in a more familiar form when the replacement $2\alpha = k\Delta R + \Delta\phi$ is substituted. Thus,

$$I = I_1 + I_2 + 2\sqrt{I_1 I_2}\cos(2\alpha)\exp\left[-\left(\frac{\alpha}{\omega\sigma_l}\right)^2\right] \qquad (22)$$

When the pulse length and coherence length are very long, the exponential factor reduces to unity, and we have the familiar two slit diffraction pattern for a monochromatic wave. The pulse length gives an amplitude modulation to the carrier wave generated by the interference term. The modulation amplitude $\exp -(\alpha/\omega\sigma_l)^2$ decays symmetrically from the center of the pattern. The arbitrary phases ϕ_1, ϕ_2 can be used to adjust the range over which the modulation is observed.

If one keeps the geometry fixed, and one compares the pattern for constant illumination (i.e., infinite pulse length) with that from a short pulse with the same irradiance, and if the ratio of the modulated parts are compared, then:

$$MR = \frac{(I-I_1-I_2)pulse}{(I-I_1-I_2)_{cw}} = \exp\left[-\left(\frac{\alpha}{\omega\sigma_l}\right)^2\right] = \exp\left[-\left(\frac{\Delta R}{2c\sigma_l}\right)^2\right] \qquad (23)$$

Then one can measure the pulse shape and pulse length simply from the MR ratio.

Two special requirements give us a guide for choosing suitable dimensions. First, a point on the screen with sufficient time delays to sample the pulse width must have enough exposure to record a signal. The slit width B should be as small as possible to spread, or diffract, the beam in order to have sufficient irradiance at that point. Second, for a given screen distance, the sampled time delay would be larger, the larger the separation between the slit. Of course, one would like to be close to the slits in order to minimize differential air disturbances and to increase the irradiance and, hence, the exposure on the screen. A reasonable choice could be made where the first minimum of the diffraction pattern from one slit ($\theta_1 = \lambda/B$) corresponds to a delay

of 3 T_p. Thus $\Delta T = 3T_p = (\lambda/\sin\theta_o)$. The diffraction pattern should be wider than the slit separation. The design of choice was B = 1 μm, λ = 0.25 μm, θ = 0.25 radian for Δt = 5 ps and A = 1200 μm. Dimensions that are hard to fabricate, but not unreasonable. Figures 2, 3, 4 and 5 show the recorded irradiance at the screen, 10 cm from the slits for illumination with 1, .5, .25, and .1 ps FWHM pulses, respectively. Only one-half of the symmetric central diffraction peak is shown. The first minima occurs at a radius 2.5 cm. The secondary fringes have lower intensity and less interest. The hatched regions in the figures are the region of modulation in the incident irradiance. The fringe separation at the screen is roughly $\lambda D/B \sim 20.8$ μm, corresponding to a 480 lpm grating. Thus these modulation are not resolvable on the scale of the plot. The lower and upper limits of the hatched regions are the limits of the modulation. The difference between these two extremes is proportional to the modulating term I_C. The dash dot central line is the incoherent sum $I_1 + I_2$ due to irradiation from the two slits. The example configuration is thus good at measuring pulses shorter than a ps. Three alternatives exist to increase the range. One reduces the slit width but with loss of signal. One can increase the slit separation, with increase in the effect of spatial coherence. Alternatively, one puts a delay in one of the paths, with a possible increase in temporal incoherence due to non-linear dispersion in the delay optics.

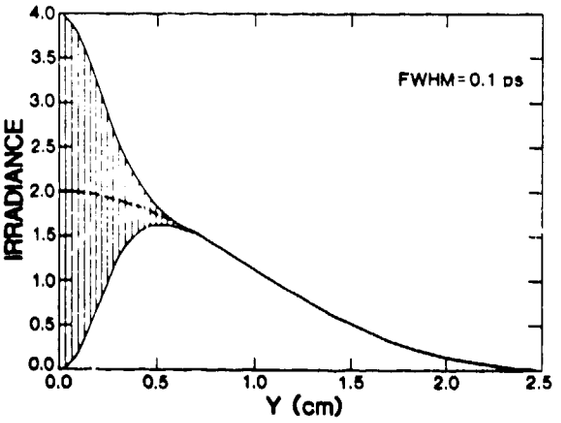

Figure 2. Irradiance as a function of axial distance along the recording plane. The hashed region represents the modulation due to interference. The interference pattern is too fine to resolve on the scale shown. The dashed curve is the result for a noncoherent super position. Each beamlet has a gaussian temporal pulse with FWHM = 0.1 ps. Slit width 1 μ, separation 1200 μ, λ = 0.25 μ.

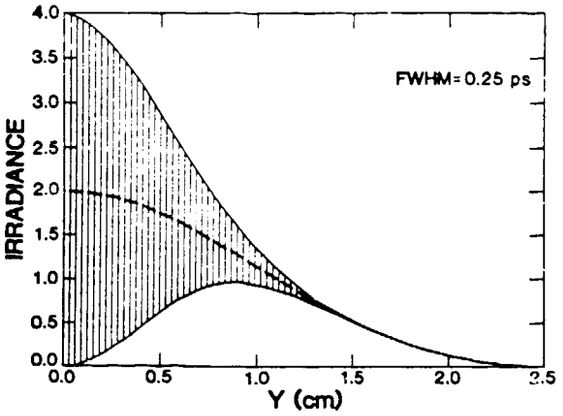

Figure 3. Irradiance as a function of axial distance along the recording plane. The hashed region represents the modulation due to interference. The interference pattern is too fine to resolve on the scale shown. The dashed curve is the result for a noncoherent super position. Each beamlet has a gaussian temporal pulse with FWHM = 0.2 ps. Slit width 1 μ, separation 1200 μ, λ = 0.25 μ.

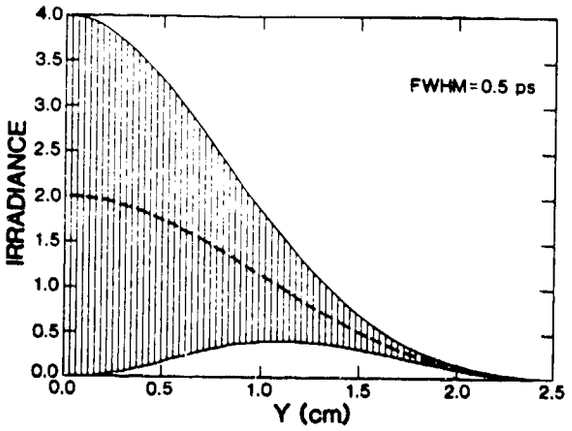

Figure 4. Irradiance as a function of axial distance along the recording plane. The hashed region represents the modulation due to interference. The interference pattern is too fine to resolve on the scale shown. The dashed curve is the result for a noncoherent super position. Each beamlet has a gaussian temporal pulse with FWHM = 0.5 ps. Slit width 1 μ, separation 1200 μ, λ = 0.25 μ.

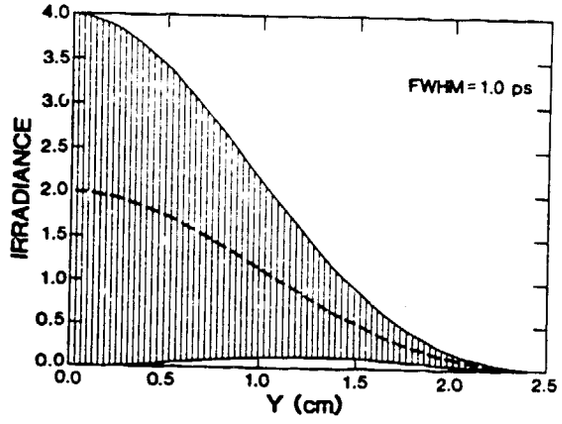

Figure 5. Irradiance as a function of axial distance along the recording plane. The hashed region represents the modulation due to interference. The interference pattern is too fine to resolve on the scale shown. The dashed curve is the result for a noncoherent super position. Each beamlet has a gaussian temporal pulse with FWHM = 1.0 ps. Slit width 1 μ, separation 1200 μ, λ = 0.25 μ.

4. SHEAR DESIGN

The shear design is based on a simple principle shown in Figure 6. The incident collimated beam gets reflected from the two surfaces of two optical flats. The two surfaces S_1 and S_2 are separated by a vertex angle α. The rays reflected from the two surfaces intersect at a point P. For collimated light, the locus of point P is a plane that intersects the surfaces S_1 and S_2 at their vertex. (For noncollimated light, the locus is a cylindrical surface.)[11] The locus plane makes an angle θ with the front surface S_1. Thus each point P on the plane corresponds to interference between rays with an optical path difference (OPD):

$$\delta = \frac{4\pi n Z}{\lambda} \tan \alpha \qquad (24)$$

where n is the index of refraction of the material between the surfaces, λ is the wavelength in vacuum, and Z is the distance from the vertex measured on the recording plane. The irradiance distribution is thus similar to that for the two slit with the replacement of the correct OPD in the formulas. Secondary reflections have been neglected in the present analysis, but can be included as in the case of a Fabry-Perot interferometer.[13]

This condition is satisfied for reflectivities of few percent from uncoated optics. The advantages of this arrangement are many. First, the nonsensitivity of the fringe location on incident angle. Second, each spatial part of the beam interfe es with itself, thus enabling spatially resolved pulse length measurement. Third, tunability of the range by changing the vertex angle α. Fourth, linearity of the Z scale with time delay or time difference. One disadvantage is the sensitivity, due to dispersion, on the index of refraction of the material through which the rays travel. This dispersion can be minimized by evacuating the region between the surfaces, and by using thin schlieren material. Another disadvantage is that the pattern is sensitive to the optical quality of the beam. The beam's wavefront differential distortion should be less than the beams pulse length if nice fringes, equidistant and parallel to the apex of the wedge, are to be observed. Any deviation will be a reflection of optical phase distortion of the incident beam.

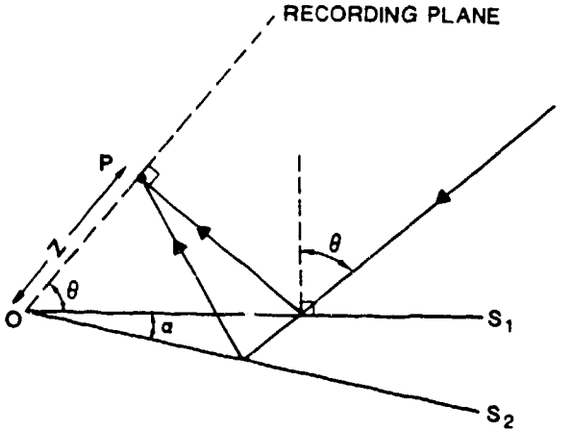

Figure 6. Geometry used for a lateral shear instruments.

By equating the geometric path difference to the delay $\Delta R = 2Z \tan \alpha = c\Delta t/n$ the dispersion of the instrument is:

$$\frac{\Delta Z}{\Delta t} = \frac{c}{2n \tan \alpha} \tag{25}$$

For a design where n=1, and a dispersion of 1 cm/ps delay then α = 15 mradian. The fringes will be separated by a distance corresponding to the propagation of one wave, i.e., $\delta = \delta + 2\pi$ using

$$\Delta\delta = \left(\frac{n4\pi \tan \alpha}{\lambda}\right)\Delta Z \tag{26}$$

then $\Delta Z = \lambda/(2n \tan\alpha) = 33\lambda/n$. For n=1, $\lambda = 1/4\ \mu$, the fringe period $\Delta Z = 8.33\ \mu$, corresponding to a 20 line per mm fringe pattern.

5. READOUT

Two methods are proposed for the readout. For ultimate resolution, each fringe should be resolved and the optical density measured. A readout beam of diameter 1 μm would easily resolve the patterns and would give sub-femptosecond resolution. For a resolution of .1 ps, a HeNe laser of roughly 1 mm readout diameter (Figure 7) would be used. The recording of the ratio of the first order versus the zero order diffraction pattern intensities would give a measure of the modulation amplitude.[14] A 1 mm diameter readout size would cover at least 100 grating cycles, enough to define the diffraction grating efficiency.

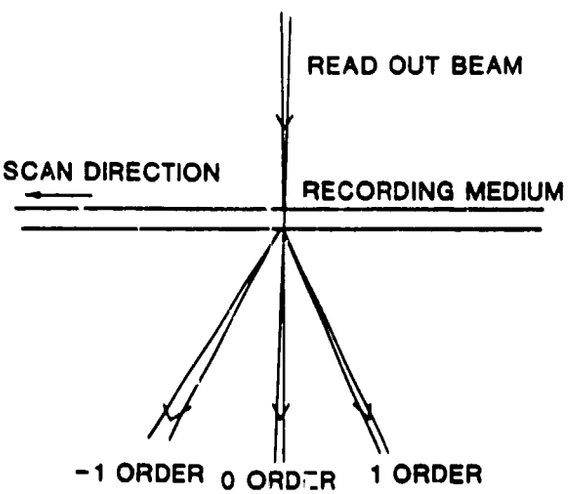

Figure 7. One proposed method for readout.

6. EFFECT OF BANDWIDTH

The theory presented so far assumes that the incident radiation is monochromatic. From the second part of this paper we associated a spectral width with the pulse width. The recorded pattern is a spectrally weighted integral over all possible frequencies within the beam. The simplest estimate for the effect of this integration can be derived from the examination of the visibility of the fringes. The visibility of the fringes will be impaired when the contribution of the mth order from one side of the spectral distribution overlaps the m $\pm$ 1 th order contribution from the other side of the spectral distribution:

$$Y_m(\lambda) = Y_{m+1}(\lambda + \Delta\lambda) \qquad (27)$$

For the two slit design, this gives m = $(\lambda + \Delta\lambda)/\Delta\lambda$. When $\Delta\lambda \ll \lambda$ this occurs at $Y_{MAX} = m\alpha\lambda/nd$ corresponding to a maximum time delay $\Delta T_{MAX} = n\Delta R/c = \lambda^2/(c\Delta\lambda)$. Substituting $\lambda\nu = c$, $c\Delta\lambda = \nu^2 d\nu$ then $\Delta T_{MAX} = 1/\Delta\nu$ which is a restatement of the uncertainty principle for measurement of complementary variables. For $\lambda = 1/4$ μm radiation from a KrF laser, $\lambda = 250$ nm and $\Delta\lambda = 1$ nm. The maximum allowed order m is less than $\lambda/\Delta\lambda = 250$. The visibility degrades at $Y_{MAX} = 520$ μm. This corresponds to a delay of 1.7 ps, sufficient to measure pulse lengths shorter than a ps. A check on this method of estimating can be done by applying it to the case of a grating. When a flat grating is illuminated by a monochromatic pulse of width W and pulse length ΔT, a finite linear extension of the grating is covered at any time. The illuminated length s = min $(c\Delta T/\sin\theta,\ W/\cos\theta)$ where θ is the angle between the normal to the grating and the direction of incidence. The maximum number of grooves covered is thus M = s/b, where b is the groove spacing. Assuming that the resolution equation for constant illumination still applies, then the measured spectrum has a resolution $\lambda/\Delta\lambda$ = mM, where m is the diffraction order.[15] Utilizing the grating formula $m\lambda = b\sin\theta$, and assuming that W is large enough not to effect the results, then $\Delta\lambda = \lambda^2/c\Delta T$. This implies $\Delta\nu\Delta T = 1$ again. Thus using a flat grating is a generalization of the two slit case, one can in principle measure the pulse length from measuring the pulse bandwidth. This, of course, applies only when the coherence length is larger than the pulse length.

7. SUMMARY

The present paper attempts to make two points. First to point out that for short pulses the coherence time is not necessarily shorter than the pulse width. Second, to present two configurations that measure the pulse shape and hence the pulse width. The two configurations rely on interference. The principles, actual design, advantages and disadvantages of the configurations were presented. The resolution and the limitations of the two methods were discussed and stated. Extensions to the multi-aperture case were also mentioned and discussed.

8. ACKNOWLEDGMENTS

The author would like to acknowledge many conversations and arguments with G. T. Schappert and J. A. Cobble. Thanks also go to Lisa Van Hecke for manuscript preparation.

8. REFERENCES

1. C. Frohly, "Traitements optiques d'impulsions laser piccoseconde," J. Opt. 12, 25-34 (1981).
2. R. Barakat, "The calculation of integrals in Optical Diffraction Theory," in The Computer in Optical Research, B. R. Friden, ed., pp. 75-78, Springer-Verlag, Berlin (1980).
3. E. P. Ippen, C. V. Shank, "Techniques for Measurement," in Ultra-Short Light Pulses, S. L. Shapiro, ed., Topics Appl. Phys. 18, Springer-Verlag, Berlin (1977).
4. M. Maier, W. Kaiser, J. A. Giordmaine, Phys. Rev. Lett. 17, 275 (1960).
5. R. L. Smith and C. O. Alley, Opt. Comm. 1, 262 (1970).
6. H. J. Eichler, U. Klein, and D. Langhans, Appl. Phys. 21, 215-219 (1980); and J. A. Cobble, Los Alamos Report No. LA-UR-86-3178.
7. J. A. Giordmaine, P. M. Rentzepis, S. L. Shapiro, and K. W. Wecht, Appl Phys. Lett. 11, 216 (1967).
8. D. C. Burnham and K. W. Billman, Appl. Phys. Lett. 13, 419 (1968).
9. O. L. Bourne and A. J. Alcock, Rev. Sci. Inst. 57, 2979 (1986).
10. M. H. R. Hutchinson, I. A. McIntyre, G. N. Gibson, and C. K. Rhodes, Opt. Lett. 12, 102 (1987).
11. M. Born and E. Wolf, Principles of Optics, p. 495, Pergamon Press, London (1984).
12. E. Hecht and A. Zajac, Optics, p. 282, Addison Wesly, Phillipines (1976).
13. E. Bernabéu, C. Rubio, and L. L. Sanchez-Soto, J. Optics (Paris) 17, 59-64 (1986).
14. D. Maystre, R. Petit, M. Duban, and J. Gilewicz, Nouv. Rev. Optique 5, No. 2, 79-85 (1974).
15. J. F. James and R. S. Sternberg, The Design of Optical Spectrometers, p. 53, Chapman and Hall, London (1969).